Rare Metal Materials and Engineering
Volume 49, Issue 6, June 2020
Available online at www.rmme.ac.cn

Science Press

Cite this article as: Rare Metal Materials and Engineering, 2020, 49(6): 1901-1906.

ARTICLE

Hydrogen Trapping and Desorption in a Martensitic Steel with Mixed (Ti,Mo)C Precipitates

Jin Xiaokun[1,2], Xu Le[1], Yu Wenchao[1] Yao Kefu[2], Shi Jie[1], Wang Maoqiu[1]

[1] Central Iron and Steel Research Institute (CISRI), Beijing 100081, China; [2] Tsinghua University, Beijing 100084, China

Abstract: Hydrogen trapping and desorption in a martensitic steel with mixed (Ti, Mo)C precipitates have been investigated by thermal desorption spectrometry (TDS) analyzer. Results indicate that the spherical (Ti, Mo)C precipitates of 36~60 nm could not absorb hydrogen during electrochemical charging, while the (Ti, Mo)C precipitates of 1~5 nm are effective hydrogen trapping sites. In spite of a relatively low desorption activation energy of 16.4~22.1 kJ/mol, which is far lower than that from pure coherent TiC, the hydrogen trapped by the fine (Ti, Mo)C carbides could not desorb during atmospheric exposure.

Key words: martensitic steel; (Ti, Mo)C precipitates; hydrogen trapping; thermal desorption spectrometry

High strength steels are usually susceptible to hydrogen embrittlement, which is one of the severe failure modes of steel components such as bolts. Precipitates such as TiC are used as hydrogen trapping sites in newly-developed high strength steels to prevent hydrogen embrittlement. It has been found that the trapping behavior of hydrogen by precipitates depends not only on the precipitate type, but also on its size, shape, and relationship with the matrix.

Precipitates can be classified into strong hydrogen trapping sites and weak hydrogen trapping sites according to the hydrogen desorption activation energy or binding energy. As for TiC precipitates, they are usually regarded as strong hydrogen trapping sites: the incoherent large TiC precipitates can have a hydrogen desorption activation energy of as high as 95 kJ/mol[1], and that of the coherent small TiC precipitates is around 40~59 kJ/mol[2,3,4]. It was reported that mixed carbides can be better than pure carbides in its ability to capture hydrogen[5]. Nagao et al[6] found that mixed nano-sized (Ti, Mo)C precipitates in a high-strength tempered lath martensitic steel increased the resistance to hydrogen embrittlement. However, there are no detail reports on hydrogen trapping at mixed (Ti, Mo)C precipitates[7]. This work is aimed to study the hydrogen trapping and desorption behavior in a martensitic steel with mixed (Ti, Mo)C precipitates.

1 Experiment

Hot-rolled wire rods with diameter of 12 mm were used in this study. The chemical composition (wt%) of the experimental steel is Fe-0.30C-0.15Si-0.31Mn-0.006P-0.002S-1.36Cr-0.18Mo-0.08Ti. The samples were first austenitized at 880 °C or 1350 °C for 5 min and oil quenched, and then tempered at different temperatures for 2 h, followed by air cooling. Three kinds of specimens, which are signified as 880/450, 1350/500, and 1350/550 by the austenitizing temperature and tempering temperature, were chosen for hydrogen trapping and desorption study, and the reason will be explained next. To distinguish different types of carbides, chemical extraction phase analyses were conducted. The content of the elements in the precipitates was measured by inductively coupled plasma-mass spectrometry (ICP-AES). Size distributions of (Ti, Mo)C particles were determined by powder X-ray diffraction-spectrometry (PANalytical X'Pert MPD)/Kratky small angle scattering goniometer with Cu Kα at 40 kV and 40 mA, according to ISO/TS13762 and GB/T 13221 standards. Scanning electron microscopy (SEM, HITACHI S-4300) and high-resolution field-emission transmission electron microscopy (HRTEM, JEM-2100F) were used to observe the microstructures and precipitates. Due to the strong magnetism of the

Received date: June 23, 2019
Foundation item: National Key Research and Development Program (2016YFB0300104, 2016YFB0300102, 2017YFB0304802)
Corresponding author: Jin Xiaokun, Candidate for Ph. D., Institute for Special Steels, Central Iron and Steel Research Institute (CISRI), Beijing 100081, P. R. China, Tel: 0086-10-62186791, E-mail: 2545835925@qq.com

sample, carbon extraction replicas were used for HRTEM observation, which were prepared by plating a carbon film of 20~30 nm thickness on the sample surface etched with 4% nital after being mechanically polished. Then, the carbon films were extracted with 4% nital and taken out with a copper net. Hydrogen was introduced by electrochemical charging using 0.1 mol/L NaOH solutions. Cylindrical samples with a diameter of 5 mm and a length of 25 mm were charged for 72 h at a current density of 0.3~3 mA/cm^2. TDS analysis was performed immediately after hydrogen charging. Details on the principle of thermal desorption analysis are available in the literature[8].

2 Results and Discussion

2.1 Microstructures and mechanical properties

The samples 880/450 and 1350/550 exhibit a typical tempered martensitic microstructure as shown in Fig.1a and 1b. The microstructure of 1350/550 is clearly coarser than that in the 880/450, due to the higher austenitizing temperature. The SEM image of 1350/500 is essentially same as that of the 1350/550.

Chemical extraction phase analysis results show that nearly all the titanium have formed MX precipitates including (Ti, Mo)C and TiN in the as-received hot-rolled wire rod. The (Ti, Mo)C particles are mainly in the range of 36~60 nm as shown in Fig.1e. According to the solid solubility product formula[9],

$$\lg[\mathrm{Ti}][\mathrm{C}] = -\frac{7000}{T} + 2.75 \quad (1)$$

when the quenching temperature is 880 °C, the (Ti, Mo)C particles formed during hot rolling will not dissolve in austenite, and thus, no new (Ti, Mo)C particles will be precipitated during the subsequent tempering process. These (Ti, Mo)C precipitates formed during hot rolling will be retained in 880/450. The TEM results show that these (Ti, Mo)C particles in the 880/450 sample are in the range of 40~60 nm, as shown in Fig.1c, which is consistent with the chemical extraction phase analysis results. The embedded figure in Fig.1c shows the selected area electron diffraction (SAED) pattern of (Ti, Mo)C particles.

When the austenitizing temperature is 1350 °C, nearly all the (Ti, Mo)C particles will dissolve in austenite. The secondary hardening platform as shown in Fig.1f implies that no new (Ti, Mo)C particles precipitated in the samples quenched at 1350 °C and tempered at 500 °C, and a large number of nano-sized (Ti, Mo)C particles newly precipitated in the steel when quenching at 1350 °C and tempering at 550 °C, as shown in Fig.1d. The chemical extraction phase analysis results also indicate that no new (Ti, Mo)C particles precipitate in the 1350/500 samples, which indicates that these MX particles of 200~300 nm must be TiN because of the higher solid solution temperature (approximately 1500 °C, Fig.1e). Small angle scattering result indicates that these newly precipitated (Ti, Mo)C particles are mainly in the size range of 1~5 nm (Fig.1e). Their components are mainly Ti, Mo, and C (Fig.1d). The main difference between the 1350/500 and 1350/550 samples is the mixed tempering (Ti, Mo)C particles of 1~5 nm, so the two samples were chosen to investigate the hydrogen trapping behavior of the mixed tempering (Ti, Mo)C carbides. The same strength, 880/450, was chosen to inves-

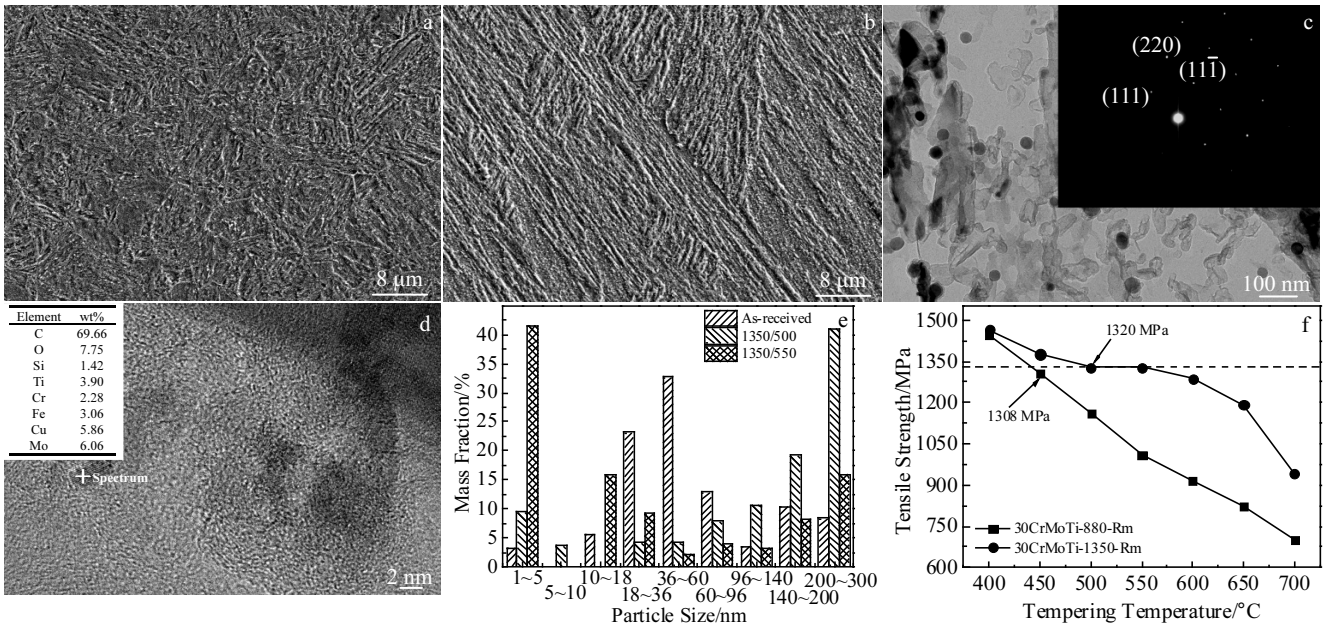

Fig.1 SEM images of 880/450 (a) and 1350/550 (b); TEM image and SAED pattern (c) of (Ti, Mo)C particles in 880/450; HRTEM image and EDS results of tempering (Ti, Mo)C particles in 1350/550 (d); particle size distribution (e); tensile strength (f)

tigate the hydrogen trapping behavior of the spherical mixed (Ti, Mo)C carbides formed during hot rolling. The detailed microstructural characteristics of the three samples are shown in Table 1.

2.2 Hydrogen trapping

Typical TDS curves of the three kinds of specimens after hydrogen charging under different current densities are shown in Fig.2. There is no significant difference before or after hydrogen charging when the heating temperature is beyond 300 °C and hydrogen introduced by electrochemical charging is mainly related to peak 1. The total content of charged hydrogen increases with increasing current density and reaches saturation when the current density is 1.2 mA/cm^2, as shown in Fig.3a. The saturated hydrogen contents of the 880/450, 1350/500, and 1350/550 samples are approximately 1, 1.5, and 3 μg/g, respectively. The saturated hydrogen content of the 1350/550 samples is approximately twice of that of the 1350/500 samples, which is presumably resulted from the trapping effect related to the mixed tempering (Ti, Mo)C precipitates with the size of 1~5 nm.

The hydrogen desorption peak temperatures of the 880/450, 1350/500, 1350/550 samples after hydrogen charging at different current densities are shown in Fig.3b. The peak temperatures tend to decrease with increasing current density. When the current density is 0.3 mA/cm^2, the peak temperature is higher than those of other current densities. It is probably due to that relatively little hydrogen is charged and these hydrogen is firstly absorbed by deeper hydrogen trapping sites that have a higher desorption temperature when the current density is 0.3 mA/cm^2. When the current density increases, the hydrogen is also charged into shallow hydrogen trapping sites. The hydrogen content tends to reach saturation, and the hydrogen desorption peak temperature is lower and stabilized at approximately 180, 163, and 145 °C for 1350/550, 1350/500, and 880/450, respectively. The hydrogen desorption peak temperature of 1350/550 is higher than that of 1350/500, indicating that the higher desorption peak temperature is attributed to the mixed tempering (Ti, Mo)C particles of 1~5 nm. When the current density is 0.3 mA/cm^2, the hydrogen is mainly in the trapping sites supplied by the tempering (Ti, Mo)C particles of 1~5 nm.

The experimental results indicate that the saturated hydrogen content of 880/450 is slightly lower than that of the 1350/500. The prior austenite grain size of 880/450 is much smaller than 1350/500 (Table 1). The hydrogen concentration in the small-grained specimens should be higher than that in the large-grained specimens due to the increase in the boundary areas, according to Chen[10]. If the undissolved (Ti, Mo)C particles of 36~60 nm could absorb hydrogen, the saturated hydrogen content of 880/450 should be higher than that of the 1350/500. It is not the case, which indicates that the spherical (Ti, Mo)C particles of 36~60 nm should be incoherent with matrix, and should not be able to absorb hydrogen through electrochemical charging under ambient temperature, according to Wei[2] and Turnbull[11]. Turnbull holds the idea that the activation energy for jumping into the trap is too high a barrier for hydrogen atoms at ambient temperature, and therefore, incoherent TiC is not an effective trap.

2.3 Hydrogen desorption and the activation energy

TDS curves of the experimental steel after saturation hydrogen charging (1.2 mA/cm^2, 72 h) and atmospheric exposure for different time (12, 24, 36, 48, 72, 96, 144 h) of

Table 1 Detailed microstructural characteristics

Specimen (heat treatment)	Prior austenite grain size/μm	Precipitates
880/450	10	M_3C + undissolved (Ti, Mo)C (36~60 nm)
1350/500	150	M_3C
1350/550	150	M_3C + Tempering (Ti, Mo)C precipitates (1~5 nm)

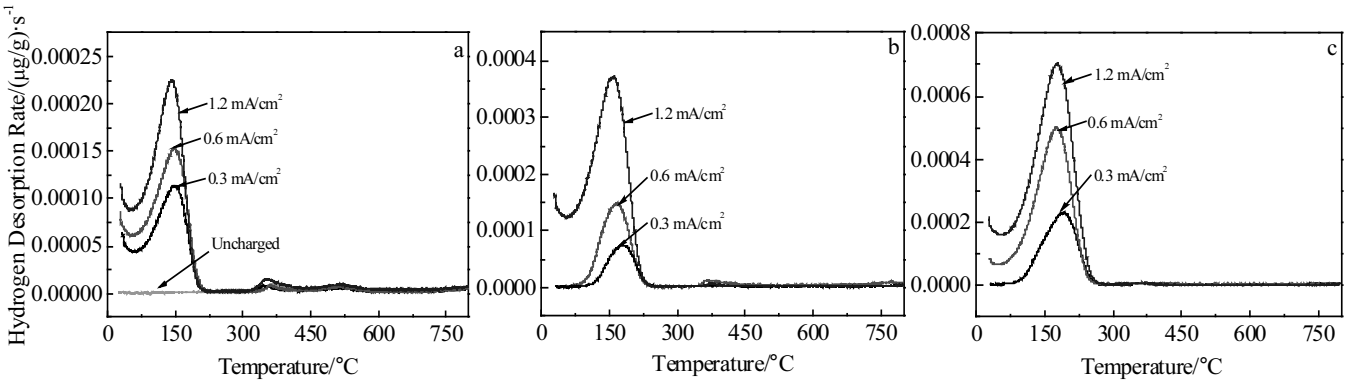

Fig.2 Typical TDS curves of the experimental steel with different heat treatment of 880/450 (a), 1350/500 (b), 1350/550 (c) after hydrogen charging under different current densities

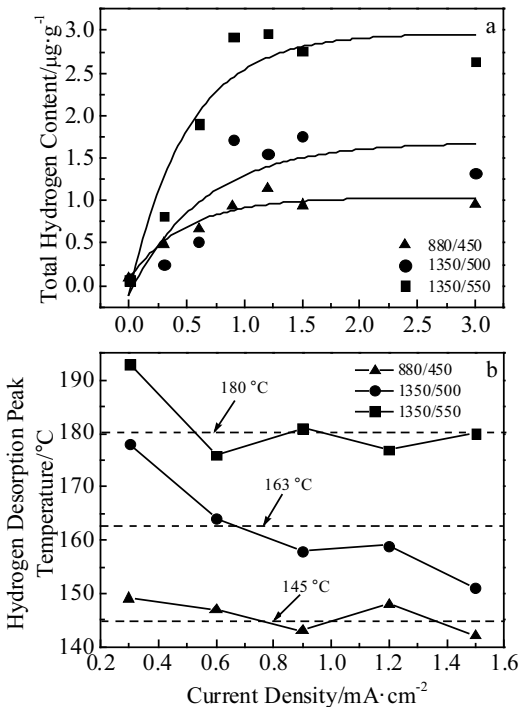

Fig.3 Variations of total hydrogen content (a) and hydrogen desorption peak temperature (b) with hydrogen charging current density

the three types of samples are presented in Fig.4.

The residual hydrogen content in the samples decreases as the exposure time increases, which essentially is unchanged when the exposure time is greater than 48 h, as shown in Fig.5a. Except for a small amount of residual hydrogen (0.5 μg/g for 1350/500, 0.3 μg/g for 880/450), the hydrogen charged into samples of 1350/500 and 880/450 through electrochemical charging basically all diffuse out after exposure for more than 72 h. However, the residual hydrogen content in the 1350/550 sample stabilizes at approximately 2.0 μg/g after saturation hydrogen charging and exposure for more than 72 h, which is more 1.5 μg/g approximately than that of the 1350/500 sample. The saturated hydrogen content of the 1350/550 sample is approximately 1.5 μg/g more than that of the 1350/500 sample without exposure, indicating that the 1.5 μg/g hydrogen is trapped by the mixed tempering (Ti, Mo)C particles of 1~5 nm. Generally, it is regarded that irreversible trapping is associated with a hydrogen desorption activation energy (E_a) of higher than 60 kJ/mol[12]. However, the experiment conducted by Depover[12] indicated that hydrogen was still present in the samples after electrochemical charging and 72 h desorption in vacuum, which can be regarded as irreversible hydrogen. The author stated that the value of 60 kJ/mol was an arbitrary choice to distinguish reversible vs. irreversible trapping sites. The 1.5 μg/g hydrogen trapped by the tempering mixed (Ti, Mo)C particles of 1~5 nm could not diffuse out upon exposure to the atmosphere, and it is irreversible according to Depover[12].

According to the diffusion model of hydrogen in long cylindrical samples[13],

$$C_t = C_\infty + 0.72(C_0 - C_\infty)\exp(-\frac{22.2D_e t}{d^2}) \quad (2)$$

The apparent diffusion coefficient of hydrogen in the three types of samples was obtained through fitting the residual hydrogen content vs atmospheric exposure time curves. The apparent diffusion coefficients of hydrogen in the 880/450, 1350/500, and 1350/550 samples are 2.6×10^{-7}, 1.1×10^{-7}, and 1.0×10^{-7} cm^2s^{-1}, respectively, as shown in Fig. 5a. It is in the same order of magnitude, and this is because the source of hydrogen diffusing out from the three types of samples is the weak hydrogen trapping sites in martensitic matrix, such as dislocation and grain boundaries. The diffusion coefficient in a martensitic structure was assumed to be approximately 4.24×10^{-7} $cm^2\cdot s^{-1}$, according to Chan[14]. There is not only one type of hydrogen trapping site in a martensitic matrix. Weakly trapped hydrogen, corresponding to a lower desorption temperature, firstly diffuses out from the samples, and therefore, the desorption peak temperature of residual hydrogen will increase with the increase of exposure time, as shown in Fig.5b. There is a small amount of hydrogen in the

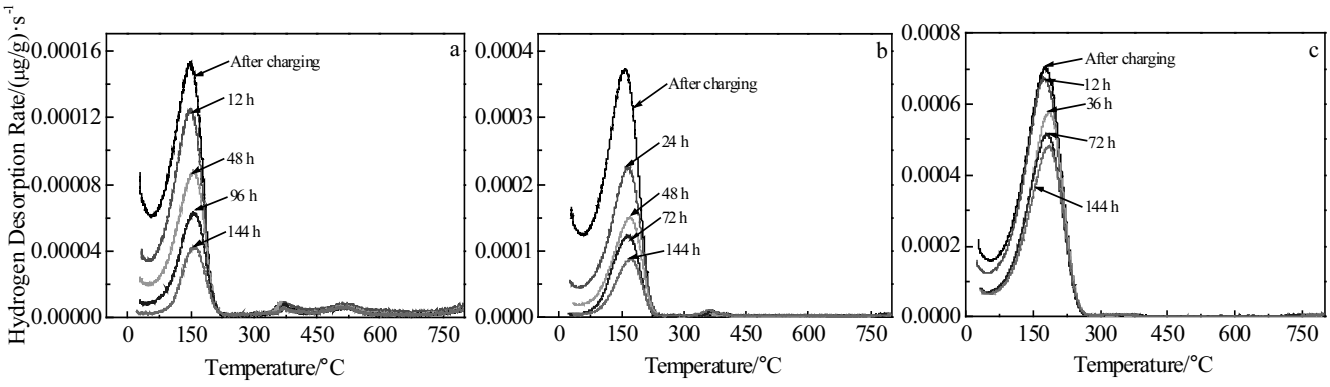

Fig.4 Typical TDS curves of the experimental steel with different heat treatment of 880/450 (a), 1350/500 (b), 1350/550 (c) after hydrogen charging at 1.2 mA/cm^2 and atmospheric exposure for different time

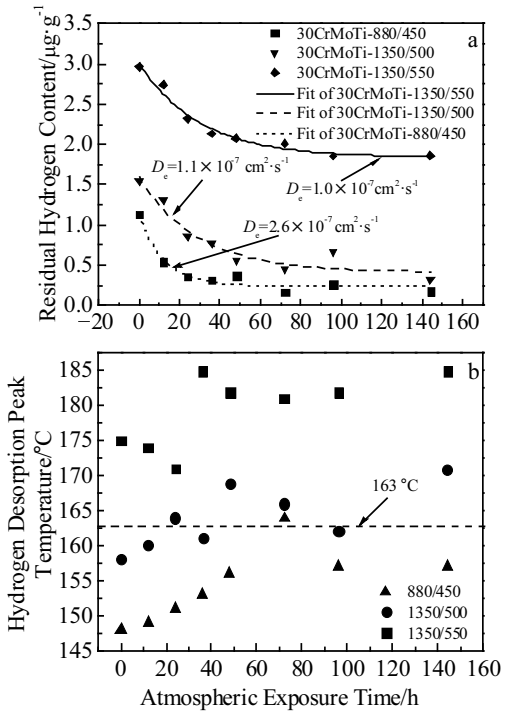

Fig.5 Variations of residual hydrogen content (a) and hydrogen desorption peak temperature (b) with atmospheric exposure time

martensitic matrix for 880/450 and 1350/500 samples when the exposure time is greater than 72 h, with the desorption peak temperature at approximately 163 °C. When the exposure time is greater than 72 h, nearly all the hydrogen in the 1350/550 sample is trapped by the tempering (Ti, Mo)C particles of 1~5 nm, which has a higher desorption peak temperature of approximately 185 °C, as shown in Fig.5b.

As previously stated, when the current density is 0.3 mA/cm^2, the hydrogen is firstly trapped by the tempering (Ti, Mo)C particles of 1~5 nm in the 1350/550 sample, and when the hydrogen is charged to saturation and exposed in the air for 96 h, the residual hydrogen is also only trapped by the tempering (Ti, Mo)C particles of 1~5 nm in the 1350/550 sample. Therefore, the hydrogen trapping activation energy, E_a, in both cases for 1350/550 was calculated. The hydrogen trapping activation energy for 880/450 and 1350/500 were also calculated according to the Choo-Lee equation[15]. Detailed information is shown in Table 2.

The calculated values of activation energy for 880/450 and 1350/500 are 16.9 and 14.7 kJ/mol, respectively. Choo and Lee[15] observed two hydrogen desorption peaks at 385 and 488 K with desorption activation energies of 17.2 and 26.8 kJ/mol, respectively, and they attributed these peaks to hydrogen trapped at grain boundaries and dislocations. Wang[16] reported that the activation energy of the measured diffusible

Table 2 Hydrogen desorption activation energy of the experimental steel

Sample	Status	Desorption peak temperature/°C				E_a/kJ·mol^{-1}
		100 °C/h	200 °C/h	300 °C/h	400 °C/h	
880/450	1.2 mA/cm^2, 72 h	148	193	226	251	16.9
1350/500	1.2 mA/cm^2, 72 h	159	210	218	282	14.7
1350/550	0.3 mA/cm^2, 72 h	193	235	263	294	22.1
1350/550	1.2 mA/cm^2, 72 h exposure for 96 h	181	235	272	302	16.4

hydrogen desorption from quenched and tempered AISI 4135 steel was 21.9 kJ/mol, and attributed this to hydrogen trapped by dislocations and grain boundaries. Wei also reported that the activation energy of hydrogen desorption from dislocation and grain boundaries in a quenched and tempered 0.05C-0.22Ti-2.0Ni steel was 21.9 kJ/mol[2]. Based on the previous research results, there was no obviously essential difference in microstructures between these studied steels, and the diffusible hydrogen desorption from 880/450 and 1350/500 samples should be trapped by dislocations and grain boundaries.

The calculated activation energy desorption from the mixed tempering (Ti, Mo)C particles of 1~5 nm (quenched at 1350 °C and tempered at 550 °C) is 16.4 and 22.1 kJ/mol for two states, which is very similar to the activation energy of diffusible hydrogen desorption from dislocations and grain boundaries as mentioned above. However, unlike hydrogen trapped by dislocations and grain boundaries that can diffuse out from the samples, hydrogen is still trapped by mixed tempering (Ti, Mo)C carbides of 1~5 nm when electrochemical charging and atmospheric exposure last for 144 h (Fig.5a).

The calculated activation energy desorption from the mixed tempering (Ti, Mo)C particles of 1~5 nm (quenched at 1350 °C and tempered at 550 °C) is 16.4 and 22.1 kJ/mol for two states, which are far smaller than the activation energy for hydrogen desorption from pure coherent TiC, 46~59 kJ/mol reported by Wei[2] and 40~50 kJ/mol reported by Depover[4]. The difference between pure TiC and mixed (Ti, Mo)C carbides is partial replacement of Ti by Mo during the formation of TiC particles. First-principles calculations[17] indicate that the replacement of Ti by Mo in the TiC lattice is energetically unfavorable with respect to the formation energy. However, it decreases the misfit strain between the carbide and ferrite matrix, which is critically important during the early stages of precipitation. Cheng et al[18] reported that the atomic ratio of Ti/Mo in the (Ti, Mo)C increased in accordance with the precipitate size in the low-carbon, low-alloy, hot-rolled sheet.

When the precipitate size grew from 5 nm to 10 nm, the atomic ratio of Ti/Mo in the precipitated phase increased from 0.53 to 1.65. The author stated that when the precipitation phase was sufficiently small, the nucleation process of (Ti, Mo)C was dominated by the interface energy, and the Mo-rich (Ti, Mo)C phase was more advantageous for reducing the interface energy. Thus, a coherent interface could be more easily formed with the matrix. In the current study, the atomic ratio of Ti/Mo in the mixed tempering (Ti, Mo)C carbides of 1~5 nm in the 1350/550 sample is approximately 1:1. Perhaps they are still in the early stage of precipitation. Partial replacement of Ti by Mo helps to decrease the strain energy and maintain a full coherent interface. Therefore, in the current study, the mixed tempering (Ti, Mo)C particles of 1~5 nm (quenched at 1350 °C and tempered at 550 °C) should be fully coherent. First-principles calculations carried out by Stefano[19] indicated that very small (<5 nm) fully coherent particles have a binding energy of <30 kJ/mol, which makes them difficult to distinguish from common crystal defects such as dislocations, grain boundaries, and other internal interfaces. Calculations conducted by Craig[20] also indicated that the interaction energy between hydrogen and a fully coherent precipitate was of the same magnitude as that calculated for hydrogen dislocation interaction. Craig[20] has drawn a conclusion that fully coherent precipitates may be hydrogen trapping sites that are as effective as dislocations, due to the elastic strain energy produced by disregistry. This is why the interaction energy between hydrogen and the mixed tempering (Ti, Mo)C carbides of 1~5 nm is similar to the activation energy of hydrogen desorption from dislocation and grain boundaries and far lower than that of pure TiC.

3 Conclusions

1) Spherical (Ti, Mo)C precipitates of 36~60 nm cannot absorb hydrogen through electrochemical charging under ambient temperature.

2) Fully coherent mixed tempering (Ti, Mo)C precipitates of 1~5 nm are effective hydrogen trapping sites with an activation energy of 16.4~22.1 kJ/mol, which is far lower than that of pure TiC and is similar to the activation energy desorption from dislocations and grain boundaries.

3) Unlike hydrogen trapped by dislocations and grain boundaries that can diffuse from of the samples, hydrogen is still trapped by mixed tempering (Ti, Mo)C carbides of 1~5 nm when electrochemical charging and atmospheric exposure last for 144 h.

References

1 Pressouyre G M, Bernstein I M. *Metall Trans A*[J], 1978, 9: 1571
2 Wei F G, Hara T, Tsuzaki K. *Metall Mater Trans B*[J], 2004, 35: 587
3 Kawakami K, Matsumiya T. *ISIJ Int*[J], 2012, 52: 1693
4 Depover T, Verbeken K. *Corros Sci*[J], 2016, 112: 308
5 Yamasaki S, Bhadeshia H K D H. *Proc R Soc A*[J], 2006, 462: 2315
6 Nagao A, Martin M L, Dadfarnia M *et al*. *Acta Mater*[J], 2014, 74: 244
7 Nagao A, Dadfarnia M, Somerday B P *et al*. *J Mech Phys Solids*[J], 2018, 112: 403
8 Wei F G, Tsuzaki K. *Metall Mater Trans A*[J], 2006, 37A: 331
9 Lee S M, Lee J Y. *Acta Metall*[J], 1987, 35: 2695
10 Chen S H, Zhao M J, Rong L J. *Mater Sci Eng A*[J], 2014, 594: 98
11 Turnbull A. *Int J Hydrogen Energy*[J], 2015, 40: 16 961
12 Depover T, Verbeken K. *Mater Sci Eng A*[J], 2016, 675: 299
13 Carneiro F C J, Mansur M B, Modenesi P J *et al*. *Mater Sci Eng A*[J], 2010, 527: 4947
14 Chan S L I. *J Inst Eng*[J], 1999, 22: 43
15 Choo W Y, Lee J Y. *Metall Trans A*[J], 1982, 13: 135
16 Wang M Q, Akiyama E, Tsuzaki K. *Mater Sci Eng A*[J], 2005, 398: 37
17 Jang J, Lee C H, Heo Y *et al*. *Acta Mater*[J], 2012, 60: 208
18 Cheng L, Cai Q W, Xie B S *et al*. *Mater Sci Eng A*[J], 2016, 651: 185
19 Stefano D D. *First-Principles Investigation of Hydrogen Interaction with Metals*[D]. Freiburg: Albert Ludwig University, 2016
20 Craig B D. *Acta Metall*[J], 1977, 25: 1027

含复合(Ti, Mo)C 析出相的马氏体钢的氢捕获与解吸附

靳晓坤[1,2]，徐　乐[1]，尉文超[1]，姚可夫[2]，时　捷[1]，王毛球[1]

(1. 钢铁研究总院，北京 100081)

(2. 清华大学，北京 100084)

摘　要：采用热脱氢分析装置 (TDS) 研究了含复合 (Ti, Mo)C 析出相的马氏体钢的氢的捕获与解吸附行为。结果表明，36~60 nm 的未溶球形(Ti, Mo)复合析出相在室温电化学充氢过程中不能捕获氢，而回火析出的 1~5 nm 的复合 (Ti, Mo)C 析出相是有效的氢陷阱，尽管其氢陷阱激活能相对较低，为 16.4~22.1 kJ/mol，与晶界、位错处的氢陷阱激活能相近，同时远低于纯的共格 TiC 析出相的氢陷阱激活能，但在大气中放置时，被回火析出的 1~5 nm 的复合 (Ti, Mo)C 析出相捕获的氢无法解吸。

关键词：马氏体钢；(Ti, Mo)C 析出相；氢陷阱；热脱氢分析

作者简介：靳晓坤，男，1987 年生，博士生，钢铁研究总院特钢所，北京 100081，电话：010-62186791，E-mail: 2545835925@qq.com